Available online at www.sciencedirect.com

SciVerse ScienceDirect

Journal of the European Ceramic Society 32 (2012) 1275–1281

www.elsevier.com/locate/jeurceramsoc

Effect of carbon content on structural and mechanical properties of SiCN by atomistic simulations

Ningbo Liao *, Wei Xue, Miao Zhang

College of Mechanical & Electrical Engineering, Wenzhou University, Wenzhou 325035, PR China

Received 6 May 2011; received in revised form 8 November 2011; accepted 19 November 2011
Available online 24 December 2011

Abstract

Silicon carbonitride (SiCN) presents good performance on thermal stability and mechanical properties at high temperature. However, experiments still have problems to investigate the chemical structure of nanodomains and high temperature mechanical properties for SiCN. In this paper, atomistic simulations were used to generate amorphous SiCN with different carbon contents, the resulting structures show a tendency to include a "free carbon" phase when the carbon content increases. The calculated pair distributions, angular distributions and structure factor are comparable with experiments. Particularly, the first peaks of C–C and Si–C distributions become more significant when C content decreases, this is related to the variations of Si–C bonds near the graphene regions when the sizes of carbon phases change. The calculated Young's moduli are close to the experimental data and increase with increasing carbon content. The proposed atomic model can be used to predict the structural and mechanical properties of SiCN at different compositions.

Keywords: Molecular dynamics; Fracture; Nanocomposites; SiC; Si_3N_4

1. Introduction

SiCN ceramics presents good performance at high temperature and has been extensively studied over the past years. The nanoscaled "free carbon" phases were found in SiCN and play a significant role in its properties. Raman spectroscopy is a main nondestructive test to study the structural evolution of the free carbon phase. Jiang[1] proposed a Raman-spectroscopy based quantitative method to measure the free carbon concentration in SiCN by using silicon as an external reference. Bragg diffraction, small-angle X-ray scattering (SAXS) and transmission electron microscopy are combined to characterize the structure of SiCN.[2] The work confirms that SiCN contains nanodomains which are 1–3 nm in size.

Although the experiments have provided some information about the structure of SiCN, it is still difficult to ascertain the chemical structure of nanodomain by microscopic and spectroscopic techniques. SAXS can provide data for the size of the domains but not the molecular structure, NMR can only give information about first nearest neighbors of molecule, and X-ray diffraction also fails as the nanodomains are not crystalline.[2] Further studies to understand the molecular structure of the domains and the domains interfaces are needed and atomistic modeling is a solution.

Amkreutz[3] modeled the atomic structure of a precursor-derived amorphous ceramic with the composition $Si_{37}C_{32}N_{31}$ by using a density-functional-based atomistic simulation. The structure factors and the pair correlation functions from X-ray and neutron diffraction were calculated and compared to the experiments. Their simulation results show a good consistence with X-ray and neutron diffraction results, while the models sizes were limited to several hundreds atoms as density-functional-based calculation is extremely time-consuming. By empirical potential and molecular dynamics, the structures of SiCN for different compositions were studied by Resta,[4] the simulations showed when stoichiometric nitrogen/silicon ratio was high enough, the amorphous ceramic separated into C-rich, SiN-rich, and SiC-rich phases. However, their models sizes were still smaller than the feature sizes of the phases in SiCN and thus the corresponding properties could not be investigated properly. Tomar[5] studied the effects of temperature and morphology on mechanical strength of SiCO and SiCN nanocomposites. Their

* Corresponding author. Tel.: +86 0577 86689138; fax: +86 0577 86689138.
E-mail address: lnb55@163.com (N. Liao).

0955-2219/$ – see front matter © 2011 Elsevier Ltd. All rights reserved.
doi:10.1016/j.jeurceramsoc.2011.11.022

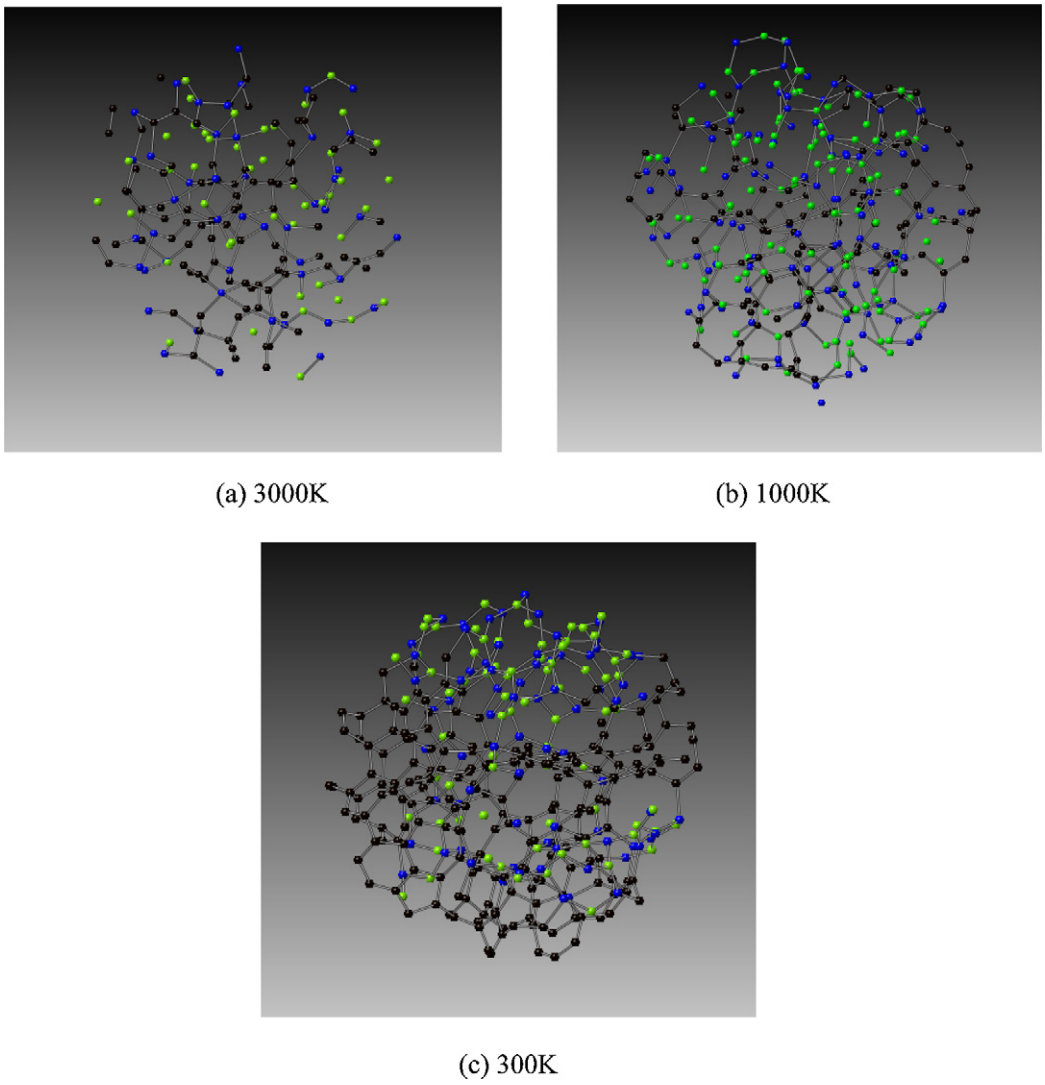

Fig. 1. Three snapshots in melt-quench process (SiC_2N): (a) 3000 K; (b) 1000 K; (c) 300 K.

SiCN structures were built up by combining Si_3N_4 matrix with SiC clusters, the results showed wall placement, wall thickness and size of nanodomain are important factors that directly affect the strength against mechanical deformation. As the morphologies are pre-designed in their models, how does the chemical composition influence these nanodomain structures should be studied further.

In this work, large-scale atomistic simulations were conducted to generate the amorphous structures of SiCN. The structures containing free carbon phases were successfully reproduced by melt-quench simulations, and then the effects of carbon content on structural and mechanical properties of SiCN were investigated.

2. Generation of amorphous SiCN

Tersoff potential[6] is used and the potential parameters for Si_3N_4 [7] and SiC[6] are combined to simulate SiCN in this study. The N–N attractive interactions in the potential energy are turned off, as there is almost no N–N bond presenting in SiCN[7,8] and this modification was successfully used in other MD simulations of SiCN.[4,9] $Si_xC_yN_z$ can partitions as Si_4CN_4 and carbon, which refers to the stoichiometric glass (50 mol% SiC and 50 mol% Si_3N_4) and excess carbon. Accordingly four SiCN models with different carbon contents were studied here: 4:1:4, 1:1:1, 1:2:1 and 1:3:1 for Si:C:N, in the order of increasing excess carbon. The models contain 100,980, 112,194, 112,396 and 129,455 atoms for Si_4CN_4, SiCN, SiC_2N and SiC_3N respectively, which correspond to 8 nm × 8 nm × 16 nm in size. Periodic boundary conditions are used in x, y and z directions. Lammps (Large-scale Atomic/Molecular Massively Parallel Simulator)[10] is used to implement the simulations, all the simulations are implemented on 24 processors of a parallel cluster.

Melt-quench technique is used to generate the amorphous structures of SiCN from random distributed atoms. Firstly the system is heat up to 8000 K for 20 ps to avoid the local energy minimum. Then it is cooled to 3000 K for 40 ps and equilibrated for 200 ps. Finally the system is cooled to 300 K for 1 ns and

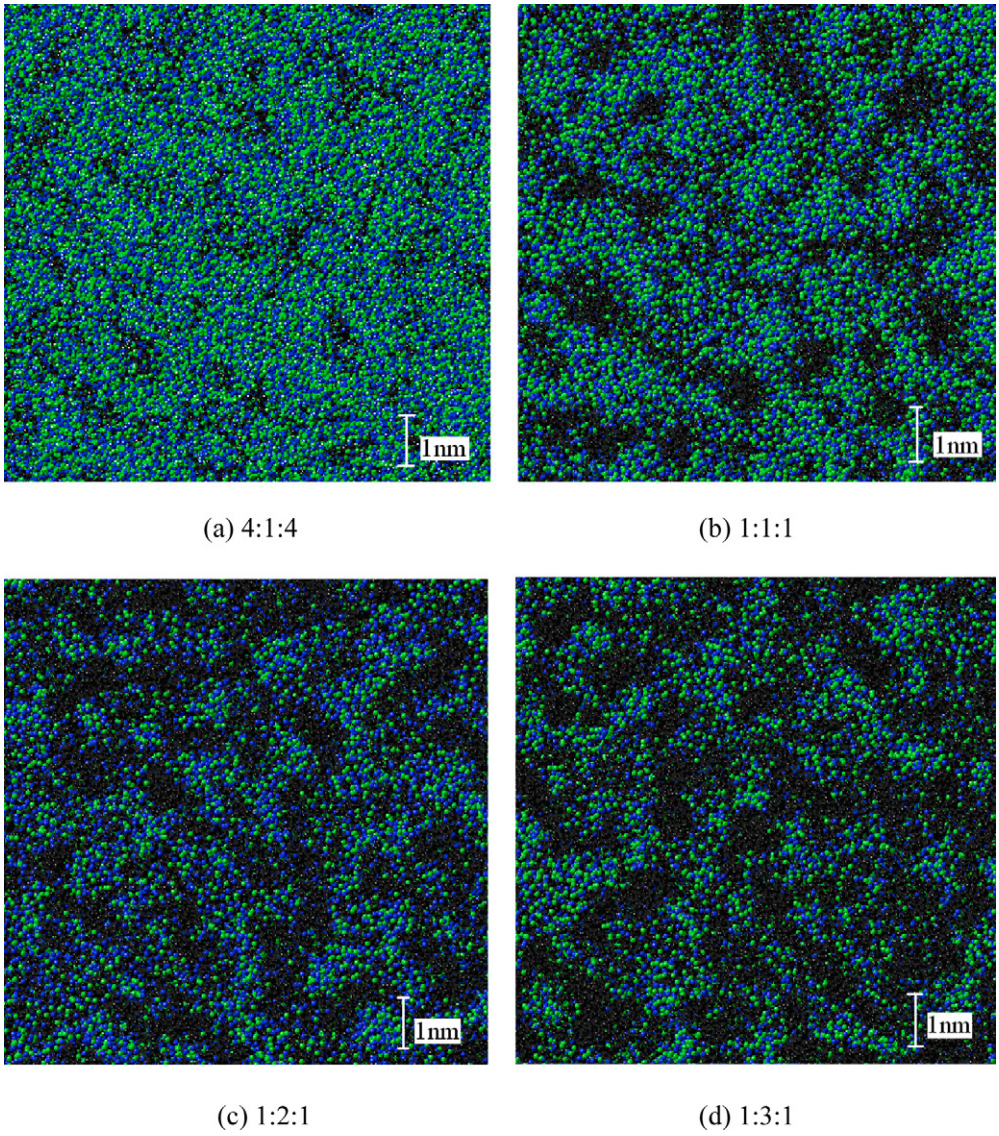

Fig. 2. Generated amorphous SiCN structures. (The Si, C and N atoms were presented as blue, black and green colors respectively.) (a) 4:1:4; (b) 1:1:1; (c) 1:2:1; (d) 1:3:1. (For interpretation of the references to color in this figure caption, the reader is referred to the web version of the article.)

equilibrated for 10 ps. Three snapshots in the melt-quench process for SiC_2N are shown in Fig. 1. It can be observed that the carbon atoms are randomly distributed at 3000 K, and tend to congregate as temperature decreases to 1000 K. When the system is cooled to 300 K, the carbon rich regions present and form interfaces with the Si–N rich regions.

The resulting structures of SiCN with different C contents are shown in Fig. 2, it can be observed that the free carbon phase presents which consists with Schempp's experimental results.[11] In Fig. 2(a), for the case with the lowest C content, i.e. the stoichiometric glass, the feature size of carbon phase is very small. With C content increases, as shown in Fig. 2(b)–(d), the carbon rich regions become larger and tend to form a network. These structures reproduce the 'nano-domain' structures of SiCN,[2] and are similar to the structures of SiCO.[12] Moreover, the sizes of carbon and Si_3N_4 regions agree with domains ranges of 1–3 nm for SiCN in SAXS experiments.[2]

3. Structural properties

The zoom in structure of the interface at carbon region and Si_3N_4 region in SiC_2N is shown in Fig. 3. It can be observed that the carbon atoms of graphitic layers only connect to silicon atoms which form mixed bonds to carbon and nitrogen atoms, and no C–N bond forms.

The atomic correlations of the SiCN structures are investigated by pair distribution functions (PDFs), which are shown in Fig. 4. The bond length of Si–N and Si–C is determined by the first sharp peaks at $r_{SiN} = 1.76$ Å and $r_{SiC} = 1.87$ Å respectively. For C–C distributions, the first peak presents at 1.48 Å, the peak is very small for high carbon model while becomes more significant when C content decreases, the similar trend is also observed in Si–C distributions. The trend relate to the Si–C correlations near the graphene regions, as the presence of carbon phase changes the Si–C bonds and the C–C bonds

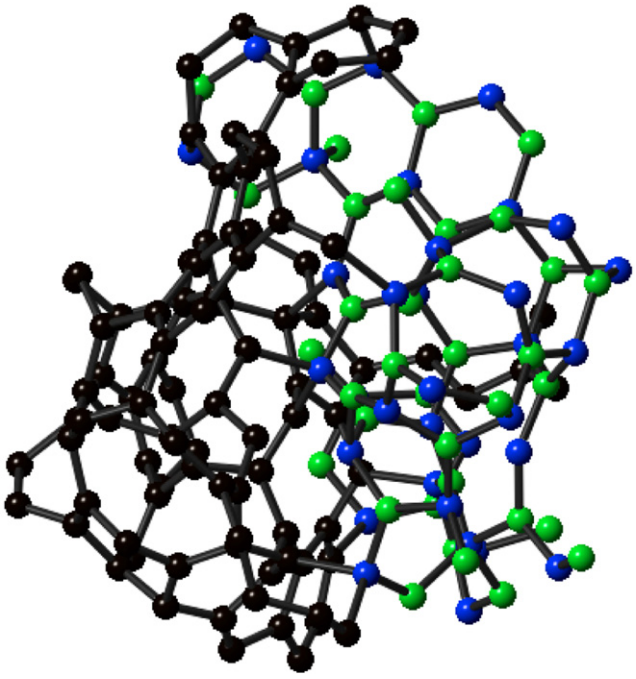

Fig. 3. Structure of carbon network in SiCN. (The Si, C and N atoms were presented as blue, black and green colors respectively.). (For interpretation of the references to color in this figure caption, the reader is referred to the web version of the article.)

are also influenced by the neighbor Si–C bonds. These PDFs results are comparable with that of DFT calculation[3] and X-ray/Neutron Diffraction experiments,[11] however, the effects of carbon content were not studied in those studies.

The static structure factor of SiCN was calculated by Fourier transform of the partial pair distribution functions, which can be directly compared to neutron and/or X-ray diffraction experiments. Fig. 5 shows the partial and total structure factors for the four compositions of SiCN. The origin of the peaks in total structure factors $S(q)$ can be inferred by means of the partial structure factors $S_{\alpha,\beta}$ (q). The peak of total $S(q)$ at 5.1 Å^{-1} is related to the short range order in real space expressed in the Si-centered tetrahedron. The peak at 2.8 Å^{-1} corresponds to real space correlation of $2\pi/q = 2.24$ Å. The peaks at lower q are responsible for the real space correlation beyond 4 Å and can be associated with an intermediate range order. The peaks positions and heights are in agreement with the experimental structure factor.[11]

Further information on the local structure is provided by the angular distribution, as shown in Fig. 6. The Si–N–Si distribution shows a peak at 119°, which is comparable with the peak at 121° for Si_3N_4 in experiments.[13] However, there is an additional peak presents at 65°, this is related to the Si–N–Si bond angle closed to the carbon regions, as the formation of Si–C bonds makes the Si–N–Si angle distorted in the interfacial regions of carbon regions and Si–N regions. The C–C–C angular distribution shows a main peak at 120°, which presents the sp^2

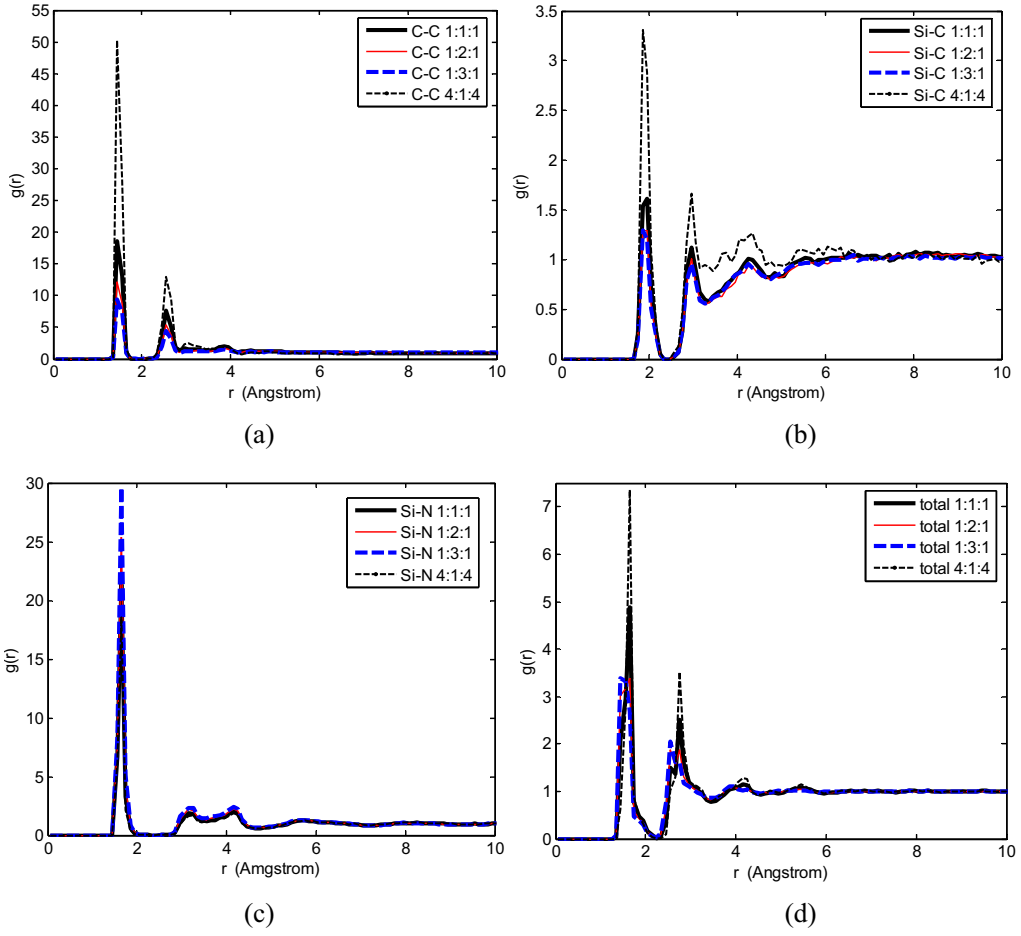

Fig. 4. Partial and total pair distribution functions for SiCN.

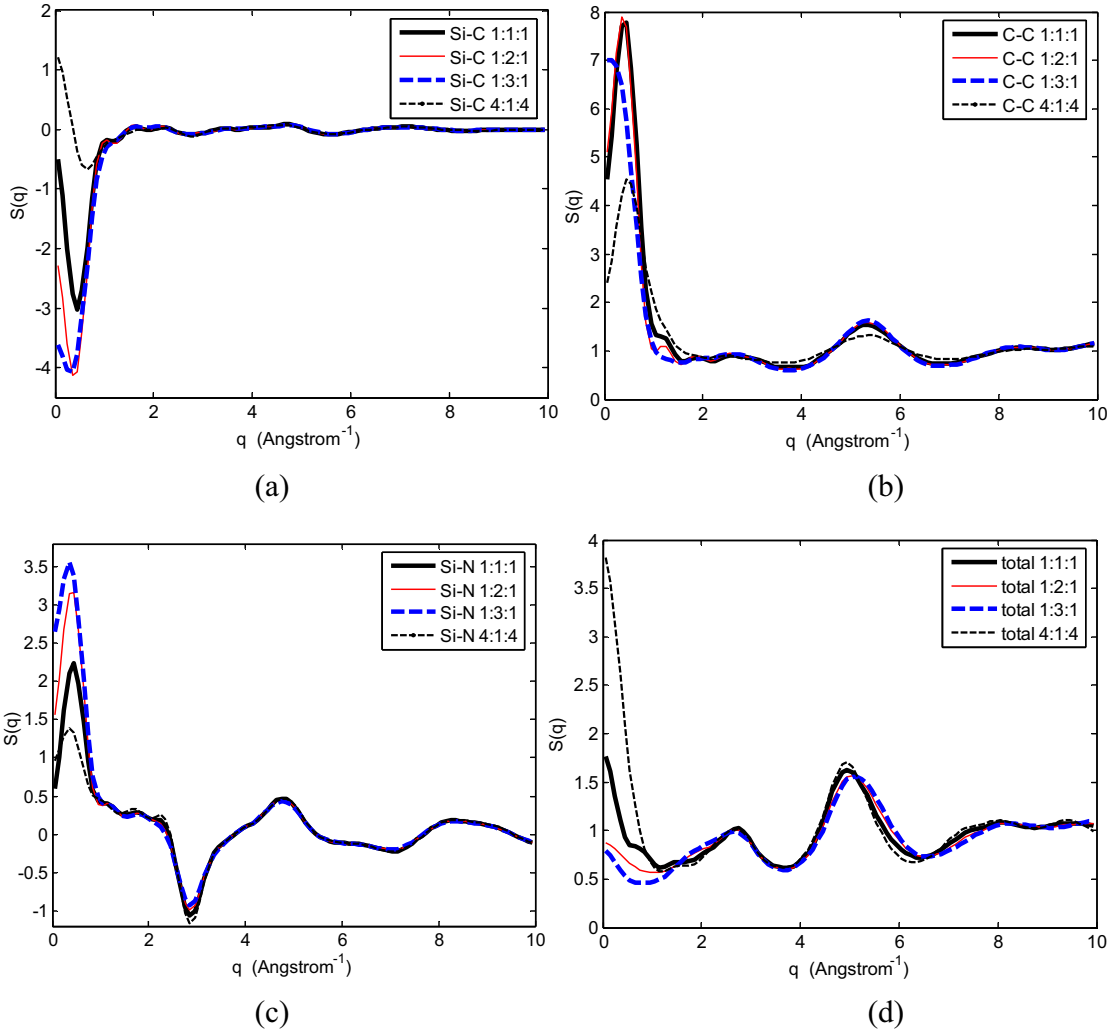

Fig. 5. Static structure factors for the three compositions of SiCN.

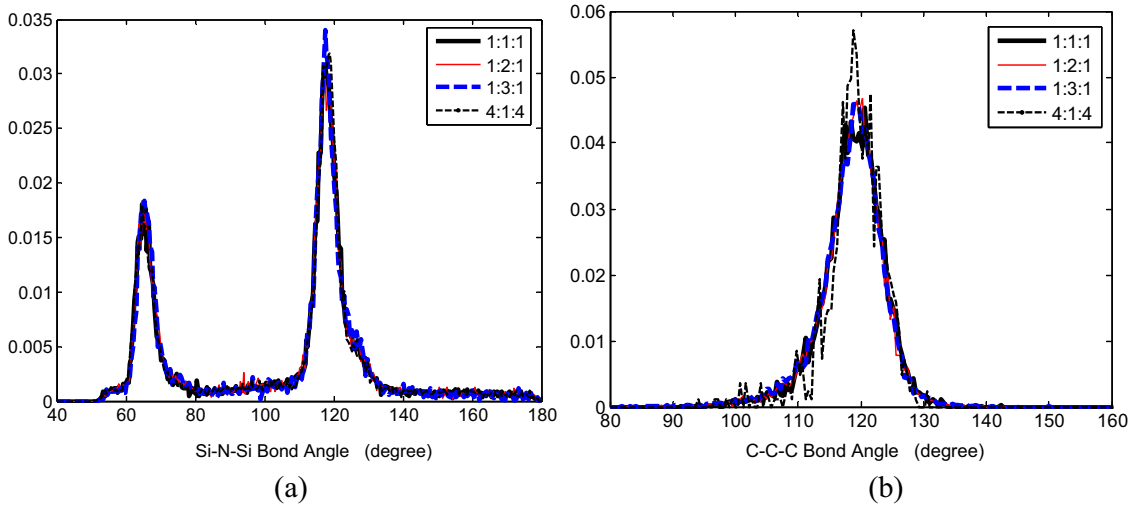

Fig. 6. Angular distributions of the SiCN structures with different carbon contents.

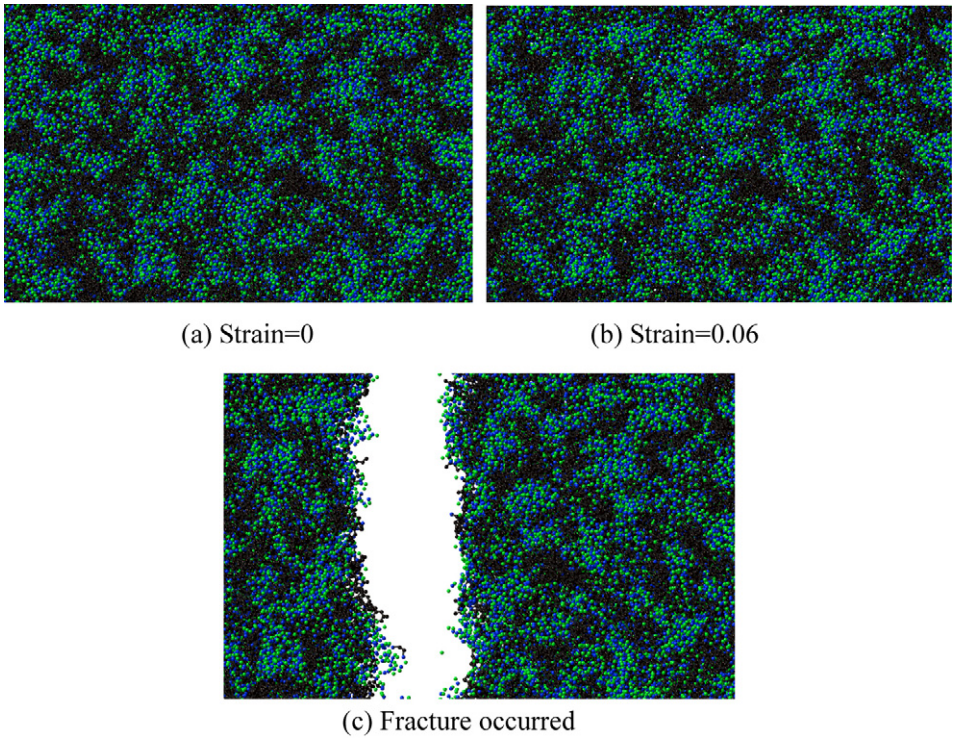

Fig. 7. Fracture process of SiCN (1:2:1) (carbon, nitrogen and silicon are shown in black, green and blue respectively). (a) Strain = 0; (b) strain = 0.06; (c) fracture occurred. (For interpretation of the references to color in this figure caption, the reader is referred to the web version of the article.)

carbon character. The peaks values of Si–N–Si distributions for different models are very close, i.e. the carbon concentration has very little influence on the angle distribution of Si–N–Si.

4. Mechanical properties

The mechanical properties were studied by tensile simulations. Periodic boundary conditions were applied to all the three dimensions. In every 10 ps, the simulation box was displaced in z direction with strain of 0.0025 and the structure was dynamically relaxed. Fig. 7 shows three snapshots in the fracture process of SiCN (1:2:1): (a) the original SiCN structure before being stretched. (b) At strain of 0.06, the structure keeps the morphology while expands in z direction, and the structure is reaching the stability limit. (c) Structure breaks suddenly. It is interesting that the fracture does not occur necessarily at the interface of Si_3N_4 region and carbon region, similar results are also observed for the other models with different C contents. While according to our current simulations of SiCO, the fracture tended to occur along the interface of SiO_2 region and carbon region. It means the interfaces between different phases are weak and act as potential fracture locations in SiCO, while the interfaces in SiCN are almost as strong as the other regions.

The Young's moduli of SiCN are calculated from the stress–strain curves of the tensile simulations. The temperature-dependent Young's modulus is shown in Fig. 8, it generally increases with an increasing carbon content and decreases with temperature increases. At room temperature, the Young's moduli ranges from 260 GPa to 280 GPa for different

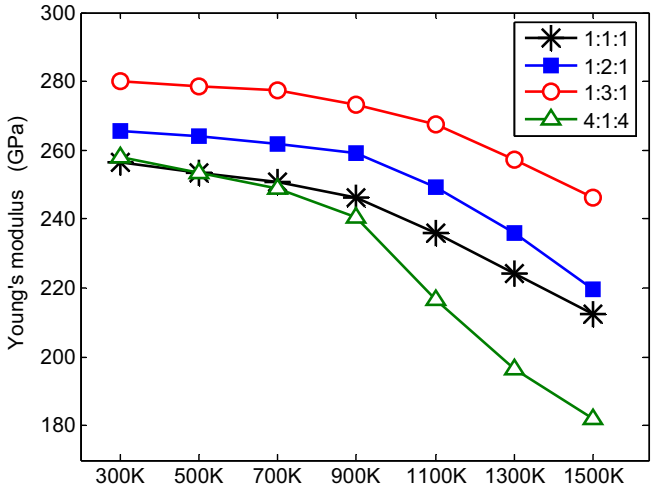

Fig. 8. Temperature-dependent Young's moduli of SiCN.

compositions, which are comparable to the range of 160–240 GPa in experiments.[14,15] However, both experiments and atomistic simulations in Ref. 14 show that the Young's modulus decreases with an increase in the carbon content in a-SiCN, which is different to our simulation results. This may be caused by several reasons: (1) the carbon contents in most of their samples are much lower, which cannot generate a large size of free carbon region. Thus the Young's modulus does not increase with an increase of carbon content. (2) DFT-based MD simulations were implemented in their study, which means very limited atoms were involved. This limitation will cause

problems in describing the carbon phase, as the feature size of carbon phase is 2–8 nm. (3) Compared with bulk materials that are studied in our simulations, their samples are deposited by ion-beam sputtering and may present different properties due to surface effects.

5. Conclusions

In this paper, atomistic simulations were conducted to study the structural and mechanical properties of silicon carbon nitride. The amorphous structures generated by melt-quench simulations reproduce the nano-domain structure of SiCN, the calculated PDFs and structure factor consist with previous DFT calculation and X-ray/Neutron Diffraction experiments. The first peaks of C–C and Si–C pair distributions are very small for high carbon model while become more significant when C content decreases, this is related to the changes in sizes of carbon phases and the corresponding variations of Si–C bonds near the graphene regions. The Young's moduli are close to the experimental data and increases with carbon content increasing. It is concluded that the fracture in SiCN does not occur necessarily at the interfaces of different phases, which means the interfaces are almost as strong as the other regions in the material.

References

1. Jiang T, Wang Y, Wang Y, Orlovskaya N, An L. Quantitative Raman analysis of free carbon in polymer-derived ceramics. *J Am Ceram Soc* 2009;**92**:2455–8.
2. Saha A, Raj R, Williamson DL, Kleebe HJ. Characterization of nanodomains in polymer-derived SiCN ceramics employing multiple techniques. *J Am Ceram Soc* 2005;**88**:232–4.
3. Marc Amkreutz, Thomas Frauenheim. Understanding precursor-derived amorphous Si–C–N ceramics on the atomic scale. *Phys Rev B* 2002;**65**:134113.
4. Resta N, Kohler C, Trebin HR. Molecular dynamics simulations of amorphous Si–C–N ceramics: composition dependence of the atomic structure. *J Am Ceram Soc* 2003;**86**:1409–14.
5. Tomar V, Gan M, Kim HS. Atomistic analyses of the effect of temperature and morphology on mechanical strength of Si–C–N and Si–C–O nanocomposites. *J Eur Ceram Soc* 2010;**30**:2223–37.
6. Tersoff J. Modeling solid-state chemistry: interatomic potentials for multicomponent systems. *Phys Rev B* 1989;**39**:5566–8.
7. Mota FDB, Justo JF, Fazzio A. Structural properties of amorphous silicon nitride. *Phys Rev B* 1998;**58**:8323–8.
8. Seher M, Bill J, Riedel R, Aldinger F. Processing and properties of carbon containing silicon nitride ceramics derived from the pyrolysis of polyhydridochlorosilazanes. *Key Eng Mater* 1994;**89–91**:101–6.
9. Matsunaga K, Iwamoto Y, Fisher CAJ, Matsubara H. Molecular dynamics study of atomic structures in amorphous Si–C–N ceramics. *J Ceram Soc Jpn* 1999;**107**:1025–31.
10. Plimpton SJ. Fast parallel algorithms for short-range molecular dynamics. *J Comp Phys* 1995;**117**:1–19.
11. Schempp S, Durr J, Lamparter P, Bill J, Aldinger F. Study of the atomic structure and phase separation in amorphous Si–C–N ceramics by X-ray and Neutron Diffraction. *Z Naturforsch A: Phys Sci* 1998;**53**: 127–33.
12. Saha A, Raj R, Williamson DL. A model for the nanodomains in polymer-derived SiCN. *J Am Ceram Soc* 2006;**89**:2188–95.
13. Misawa M, Fukinga T, Nihara K, Hirai T, Suzuki K. Structure characterization of CVD amorphous Si_3N_4 by pulsed neutron total scattering. *J Non-Cryst Solids* 1979;**34**:313–21.
14. Lehmann G, Hess P, Wu JJ, Wu CT, Wong TSS, Chen KH, et al. Structure and elastic properties of amorphous silicon carbon nitride films. *Phys Rev B* 2001;**64**:165305.
15. Awad Y, Khakani MAE, Aktik C, Mouine J, Camiré N, Lessard M, et al. Structural and mechanical properties of amorphous silicon carbonitride films prepared by vapor-transport chemical vapor deposition. *Surf Coat Technol* 2009;**204**:539–45.